

Article

# A Tabu-Matching Heuristic Algorithm Based on Temperature Feasibility for Efficient Synthesis of Heat Exchanger Networks

Xiaohuang Huang, Hao Shen, Wenhao Yue, Huanhuan Duan and Guomin Cui \*

Shanghai Key Laboratory of Multiphase Flow and Heat Transfer in Power Engineering,  
School of Energy and Power Engineering, University of Shanghai for Science and Technology,  
Shanghai 200093, China

\* Correspondence: cgm@usst.edu.cn

**Abstract:** The non-structural model of heat exchanger networks (HENs) offers a wide solution space for optimization due to the random matching of hot and cold streams. However, this stochastic matching can sometimes result in infeasible structures, leading to inefficient optimization. To address this issue, a tabu matching based on a heuristic algorithm for HENs is proposed. The proposed tabu-matching method involves three main steps: First, the critical temperature levels—high, medium, and low-temperature intervals—are determined based on the inlet and outlet temperatures of streams. Second, the number of nodes is set according to the temperature intervals. Third, the nodes of streams are flexibly matched within the tabu rules: the low-temperature interval of hot streams with the high-temperature interval of cold streams; the streams crossing cannot be matched. The results revealed that by incorporating the tabu rules and adjusting the number of nodes, the ratio of the feasible zone in the whole solution domain increases, and the calculation efficiency is enhanced. To evaluate the effectiveness of the method, three benchmark problems were studied. The obtained total annual costs (TACs) of these case studies exhibited a decrease of USD 4290/yr (case 1), USD 1435/yr (case 2), and USD 11,232/yr (case 3) compared to the best published results. The results demonstrate that the proposed tabu-matching heuristic algorithm is effective and robust.

**Keywords:** heat exchanger network; heuristic method; temperature interval; tabu matching



**Citation:** Huang, X.; Shen, H.; Yue, W.; Duan, H.; Cui, G. A Tabu-Matching Heuristic Algorithm Based on Temperature Feasibility for Efficient Synthesis of Heat Exchanger Networks. *Processes* **2023**, *11*, 2713. <https://doi.org/10.3390/pr11092713>

Academic Editors: Wei Li, Weiyu Tang, Junye Li and David Kukulka

Received: 9 August 2023  
Revised: 5 September 2023  
Accepted: 8 September 2023  
Published: 11 September 2023



**Copyright:** © 2023 by the authors. Licensee MDPI, Basel, Switzerland. This article is an open access article distributed under the terms and conditions of the Creative Commons Attribution (CC BY) license (<https://creativecommons.org/licenses/by/4.0/>).

## 1. Introduction

With the continuous depletion of fossil energy resources and growing concerns about global warming, the energy crisis has emerged as one of the most pressing concerns in today's global economy. Heat exchangers are significant elements within a thermal system [1], where some heat exchangers are organized to operate as heat exchanger networks (HENs) to recover waste heat and lower overall energy consumption. Solving the HEN synthesis problem involves dealing with both integer variables (e.g., stream matches) and continuous variables (e.g., heat exchanger load and stream split fractions). Accordingly, this problem can be categorized as a mixed-integer nonlinear programming problem. Moreover, the research on HEN synthesis can be extended to tackle optimization problems in domains closely related to system integration. These domains include the synthesis of mass exchange networks [2], hydrogen distribution networks [3], water networks [4], and transmission and distribution networks [5–7]. Hence, the global optimization of the HEN synthesis problem is considered a challenging and hot research topic in the field of process system integration.

In this context, pinch point techniques [8,9], deterministic methods [10,11], and heuristic methods [12–15] have been successively applied to HEN synthesis. Recently, Fu et al. [16] used pinch analysis in the shifted temperature driving force plot to improve energy recovery and economic benefits in the transformation of HENs. Orosz et al. [17] proposed a heuristic framework for selecting the best structural parameters via an extension of the P-HEN synthesis solver. Lakner et al. [18] modified the P-graph-based HEN synthesis

method and proposed a procedure for HEN synthesis that determines the best, n-best, or all feasible HENs for all periods, considering variable approach temperatures. It is worth noting that the aforementioned methods achieved reasonable optimization results.

The models of HEN synthesis serve as the foundation for synthesis and are designed to streamline algorithm implementation and result representation. The stage-wise superstructure (SWS) model [19] is one of the most widely used models. The SWS model contains most structures and can achieve reasonable solutions in various case studies and scenarios. However, some heat exchange patterns in SWS are not feasible [19]. Numerous models [20–23] have been proposed to bolster the model's adaptability and broaden its solution scope to enhance its practical problem-solving capacity. Xiao [24] proposed a non-structural model (NSM) without frame constraints, different from the constraints of the SWS model. The proposed model uses nodes on the streams as connection points for the heat exchanger units. During optimization, the hot and cold nodes can be freely matched, enabling a more accessible and flexible matching design and ensuring a sufficient solution space.

From the thermodynamic standpoint, the random nature of mode matching in the NSM model may yield infeasible structures, such as heat exchanger units with temperature crossover or heat transfer from a low-temperature stream to a high-temperature stream. Researchers [25–27] introduced penalty functions to avoid impractical structures. These functions are added to the objective function when constraints are violated. This approach does not prevent the generation of infeasible solutions but directs the network population to the feasible domain with high probability, thereby effectively preventing infeasible solutions. However, only a few studies have approached the issue from the perspective of narrowing down the infeasible domains.

This paper introduces a temperature interval tabu matching of the Random Walk algorithm with Compulsive Evolution (RWCE-TB) to eliminate infeasible matching structures while preserving valuable iterations and discarding ineffective ones, thereby improving the optimization quality. The method is based on the concept of locating the temperature interval for each process stream, namely high, medium, or low-temperature intervals. Then, the number of nodes is set according to the temperature intervals. Since calculating each HEN involves traversing all predefined nodes in the NSM model, the configuration of nodes affects the efficiency of optimization. The NSM typically assigns an equal number of nodes to both hot and cold streams. However, streams with larger temperature spans can lead to more diverse matching relationship situations. Hence, it is essential to adjust the allocation of nodes accordingly. This adjustment ensures an adequate number of nodes for streams with larger temperature spans, preventing the issue of insufficient nodes, which may hinder the flexible insertion of new stream matches. Conversely, for streams with smaller temperature spans, the number of nodes should be reduced appropriately to avoid the unnecessary waste of nodes and reduce computation time caused by an excessive number of nodes. Finally, a tabu matching is proposed based on temperature intervals. Specific matches are considered "forbidden" or "restricted" to eliminate infeasible matching structures in tabu matching. The nodes of streams are flexibly matched, but the following nodes are in the tabu rules, which cannot be matched: the nodes on the low-temperature interval of hot streams with that on the high-temperature interval of cold streams, and the nodes on the streams that are temperature crossings.

The remainder of this article is organized as follows: The HEN synthesis problem, the NSM, the objective function, and constraints are introduced in Section 2. In Section 3, the RWCE is utilized to solve the problem, the infeasible matching structures in the NSM with RWCE and their adverse effects on the optimization are discussed, and then the heuristic optimization method for tabu matching the temperature intervals of HEN synthesis is introduced. In Section 4, the established method is employed in three test cases to verify its effectiveness. Finally, the main achievements are summarized in Section 5.

## 2. Model Formulation

### 2.1. Problem Statements

In a chemical process,  $N_H$  hot streams require cooling, and  $N_C$  cold streams need to be heated. To this end, multiple heat exchangers are designed to facilitate heat recovery from the hot streams and utilize the absorbed heat in the cold streams. The design involves various parameters, including the inlet and outlet temperatures of the streams, heat capacity flow rate, and convective heat transfer coefficient. This arrangement forms a HEN. In cases where heat recovery alone cannot reach the desired target temperature, additional hot and cold utilities are necessary, consuming extra hot and cold sources. Typically, saturated steam and cooling water are commonly chosen as the hot and cold utilities, respectively, due to their known inlet and outlet temperatures and heat transfer coefficients. These utilities are used to either heat the cold process streams or cool the hot process streams to the target temperature. The primary goal of HEN synthesis is to enhance system energy efficiency or reduce investment costs.

### 2.2. Non-Structural Model

Xiao et al. [24] introduced a widely used NSM for the HEN synthesis problem. This model offers significant freedom and randomness, which contributes to expanding the solution domain and obtaining global optimal solutions. The NSM constructs heat exchanger units through node connections, resulting in a highly flexible matching of heat exchanger units and ensuring optimization continuity. This characteristic allows for the generation of diverse potential network structures.

Figure 1 illustrates a schematic diagram of an example, labeled as H2C2. “H” and “C” signify hot and cold streams, respectively; the subsequent numerical values indicate the number of hot and cold streams. Specifically, H2C2 consists of  $N_H = 2$  hot streams and  $N_C = 2$  cold streams. In Figure 1, each horizontal line with arrows represents a stream, whereas the red and blue lines represent hot and cold streams. The arrows indicate the flow direction of the streams. Along each stream, hollow dots represent nodes where heat exchanger units can be located. At the end of the streams, a C in a blue hollow dot and an H in a red one indicate cold and hot utility, respectively. A set of solid nodes connected by a black straight line represents the presence of a heat exchanger unit at that specific location of a hot and cold node. In this example, the number of hot stream nodes per stream is set to  $N_{dH} = 3$ , and the number of cold stream nodes per stream is set to  $N_{dC} = 3$ . There are four heat exchanger units indicated by these solid nodes.

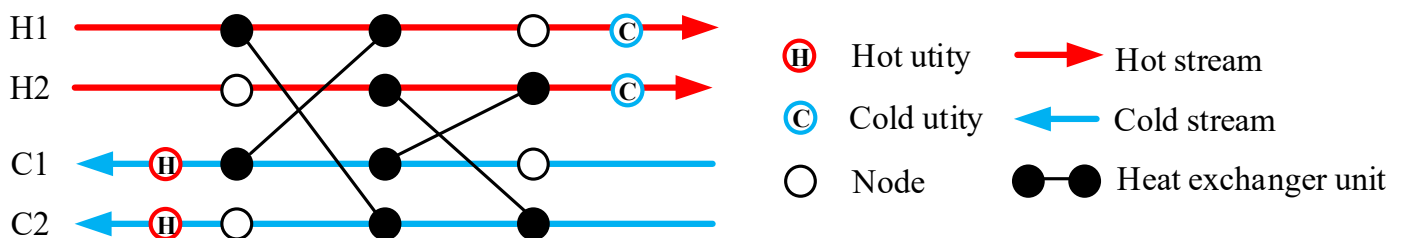


Figure 1. Schematic diagram of the NSM.

### 2.3. Objective Function

The optimization objective of the HEN in this work is to minimize the TAC, which can be expressed as follows:

$$\min TAC = \sum_{n_{bH}=1}^{N_{bH}} (F_{\text{Fix}} + C_A \cdot A_{n_{bH}}^\epsilon) \cdot X_{n_{bH}} + \sum_{i=1}^{N_H} (F_{\text{Fix}} + C_A \cdot A_{\text{CU},i}^\epsilon) \cdot X_{\text{CU},i} + \sum_{j=1}^{N_C} (F_{\text{Fix}} + C_A \cdot A_{\text{HU},j}^\epsilon) \cdot X_{\text{HU},j} + \sum_{i=1}^{N_H} (C_{\text{CU}} \cdot Q_{\text{CU},i}) \cdot X_{\text{CU},i} + \sum_{j=1}^{N_C} (C_{\text{HU}} \cdot Q_{\text{HU},j}) \cdot X_{\text{HU},j} \quad (1)$$

where  $N_H$  and  $N_C$  are the number of hot and cold streams, respectively. Variable  $X$  is a binary variable that can take the value 0 or 1. When  $X$  equals 1, it indicates the presence of a heat exchanger or cold and hot utility at the corresponding nodes. On the other hand, when  $X$  is 0, the nodes are empty without any units.  $F_{\text{fix}}$  is the fixed investment cost,  $C_A$  is the area cost coefficient, and  $n_{\text{bH}}$  is the serial number on the hot stream nodes.  $\varepsilon$  is the area cost index, and  $C_{\text{CU}}$  and  $C_{\text{HU}}$  are the coefficients of the operating cost of cold and hot utilities, respectively.  $A_{n_{\text{bH}}}$ ,  $A_{\text{CU},i}$ , and  $A_{\text{HU},j}$  are the areas of heat exchanger unit, cold utility, and hot utility, respectively. Meanwhile,  $Q_{\text{CU},i}$  and  $Q_{\text{HU},j}$  are the consumption heat loads of cold and hot utilities, respectively. The first three items in the equation represent the fixed investment and area costs associated with the heat exchanger units and the cold and hot utility equipment. On the other hand, the last two items represent the energy consumption costs incurred by the cold and hot utilities. The TAC is also related to the area of heat exchangers, which can be expressed as follows:

$$A_{n_{\text{bH}}} = \frac{Q_{n_{\text{bH}}}}{U_{i,j} \cdot \text{LMTD}_{n_{\text{bH}}}}, i \in N_H, j \in N_C, n_{\text{bH}} \in N_{\text{bH}} \quad (2)$$

$$U_{i,j} = \frac{h_i \cdot h_j}{h_i + h_j}, i \in N_H, j \in N_C \quad (3)$$

$$\text{LMTD}_{n_{\text{bH}}} = \begin{cases} \frac{(T_{n_{\text{bH}}}^{\text{in}} - T_{\text{MC}(n_{\text{bH}})}^{\text{out}}) - (T_{n_{\text{bH}}}^{\text{out}} - T_{\text{MC}(n_{\text{bH}})}^{\text{in}})}{\ln\left(\frac{T_{n_{\text{bH}}}^{\text{in}} - T_{\text{MC}(n_{\text{bH}})}^{\text{out}}}{T_{n_{\text{bH}}}^{\text{out}} - T_{\text{MC}(n_{\text{bH}})}^{\text{in}}}\right)}, T_{n_{\text{bH}}}^{\text{in}} - T_{\text{MC}(n_{\text{bH}})}^{\text{out}} \neq T_{n_{\text{bH}}}^{\text{out}} - T_{\text{MC}(n_{\text{bH}})}^{\text{in}} \\ \frac{(T_{n_{\text{bH}}}^{\text{in}} - T_{\text{MC}(n_{\text{bH}})}^{\text{out}}) + (T_{n_{\text{bH}}}^{\text{out}} - T_{\text{MC}(n_{\text{bH}})}^{\text{in}})}{2}, T_{n_{\text{bH}}}^{\text{in}} - T_{\text{MC}(n_{\text{bH}})}^{\text{out}} = T_{n_{\text{bH}}}^{\text{out}} - T_{\text{MC}(n_{\text{bH}})}^{\text{in}} \end{cases} \quad (4)$$

where  $U_{i,j}$  is the total heat transfer coefficient,  $h$  is the convective heat transfer coefficient of the stream, and  $\text{LMTD}$  is the logarithmic mean temperature difference. When the heat transfer temperature difference between the left and right ends of the heat exchanger unit is less than  $10^{-5}$  °C, the arithmetic mean temperature difference is used instead of the logarithmic mean temperature difference. The superscripts “in” and “out” indicate the inlet and outlet, respectively. The subscripts  $i$  and  $j$  represent the  $i_{\text{th}}$  hot stream and  $j_{\text{th}}$  cold stream, respectively.  $\text{MC}(n_{\text{bH}})$  is the serial number of the cold node connected with the hot stream node  $n_{\text{bH}}$ .

#### 2.4. Constraints

For each HEN structure, the following constraints should be satisfied:

- (i) Overall heat balance in each stream

$$(T_{H,i}^{\text{in}} - T_{H,i}^{\text{target}}) \cdot F_{\text{CP},i} = \sum_{n_{\text{dH}}=1}^{N_{\text{dH}}} Q_{H,i,n_{\text{dH}}} + Q_{\text{CU},i}, i \in N_H \quad (5)$$

$$(T_{C,j}^{\text{target}} - T_{C,j}^{\text{in}}) \cdot F_{\text{CP},j} = \sum_{n_{\text{dC}}=1}^{N_{\text{dC}}} Q_{C,j,n_{\text{dC}}} + Q_{\text{HU},j}, j \in N_C \quad (6)$$

where  $N_{\text{dH}}$  and  $N_{\text{dC}}$  are the number of nodes on each hot and cold stream, respectively.

- (ii) Temperature constraints

The temperature should satisfy the following constraints to prevent the temperature crossing and infinite exchanger area:

$$T_{n_{\text{bH}}}^{\text{in}} - T_{\text{MC}(n_{\text{bH}})}^{\text{out}} \geq \Delta T_{\text{min}} \quad (7)$$

$$T_{n_{\text{bH}}}^{\text{out}} - T_{\text{MC}(n_{\text{bH}})}^{\text{in}} \geq \Delta T_{\text{min}} \quad (8)$$

$$T_{N_{dH},i}^{\text{out}} - T_{CU,i}^{\text{out}} \geq \Delta T_{\min} \quad (9)$$

$$T_{H,i}^{\text{target}} - T_{CU,i}^{\text{in}} \geq \Delta T_{\min} \quad (10)$$

$$T_{HU,j}^{\text{in}} - T_{C,j}^{\text{target}} \geq \Delta T_{\min} \quad (11)$$

$$T_{HU,j}^{\text{out}} - T_{L,j}^{\text{in}} \geq \Delta T_{\min} \quad (12)$$

where  $\Delta T_{\min}$  is the minimum approach temperature.

### 3. Solution Approach

This section focuses on the RWCE approach in solving the HEN synthesis problem using the NSM model, addressing infeasible matching structures and their optimization-related consequences. Subsequently, the implementation of RWCE with tabu matching (RWCE-TB) is discussed.

#### 3.1. Random Walk Algorithm with Compulsive Evolution

Figure 2 depicts the detailed flowchart of the RWCE, a simultaneous heuristic approach used for the global optimization of HEN issues [15]. This method leverages the principles of the random walk algorithm, which allows for the simultaneous optimization of integer and continuous variables. The optimization process involves randomly adjusting the heat loads of the heat exchangers. The critical optimization steps within RWCE include initialization, evolution, generation, selection, and mutation. Importantly, RWCE incorporates a probability mechanism that allows for accepting imperfect solutions, which helps prevent the algorithm from getting trapped in local optima and improves the chances of finding global optima.

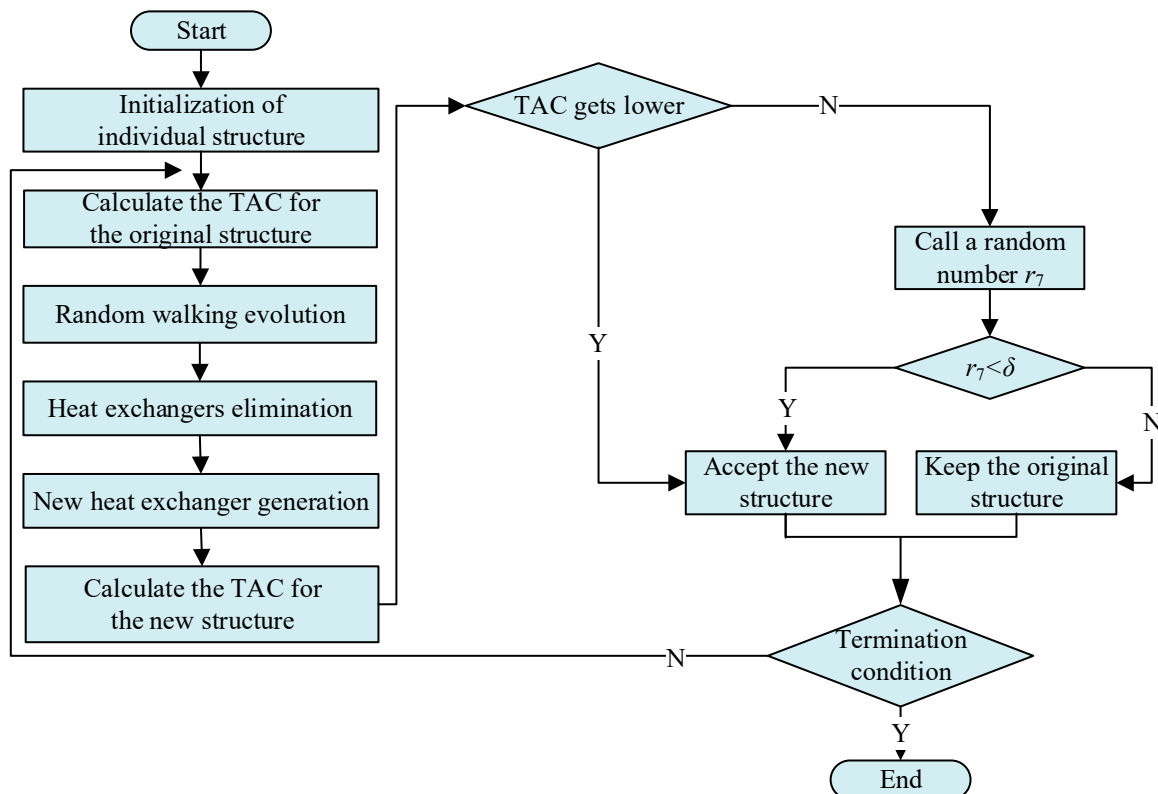


Figure 2. Flowchart of the RWCE algorithm.

(1) Initialization of individual structure

In the RWCE optimization approach, the HEN is represented by a population of  $N$  individuals ( $n = 1, 2, \dots, N$ ). Each individual in the population is a potential HEN structure. During the initialization phase, the HEN's design is set to be empty, with nodes left unconnected. Consequently, the streams within the HEN initially rely on energy from the utilities to reach their desired target temperatures.

(2) Random walking operation

A random evolutionary process of the heat loads is performed in a HEN structure, specifically for the existing heat exchanger units. This process is governed by an evolution probability denoted as  $\phi$ . This can be mathematically expressed in the form below:

$$(Q'_{n_{bH}})_{it+1} = \begin{cases} (Q_{n_{bH}})_{it} + (1 - 2\rho) \cdot \Delta L \cdot \beta \cdot \omega_1 & , \text{ if } r_1 < \phi \\ (Q_{n_{bH}})_{it} & , \text{ otherwise} \end{cases} \quad (13)$$

where  $Q_{it}$  and  $Q_{it+1}$  are the heat load of the heat exchanger unit at iteration ' $it$ ' and the heat load of the same heat exchanger unit after undergoing a random walk. The parameters  $\rho$ ,  $\beta$ , and  $\omega_1$  are random numbers within the range of (0, 1). Moreover,  $\Delta L$  determines the maximum step size during evolution, while  $(1 - 2\rho)$  determines the direction of movement in each dimension in each individual evolution.

(3) Heat exchanger elimination

When the heat load of a heat exchanger unit falls below the threshold value  $Q_{\min}$  after the random walking process, this indicates that the heat exchanger is not operating efficiently. In such cases, the heat exchanger will be forcibly eliminated from the network, and its original node connection relationship will be removed.

$$Q''_{n_{bH}} = \begin{cases} Q'_{n_{bH}} & , \text{ if } Q'_{n_{bH}} > Q_{\min} \\ 0 & , \text{ otherwise} \end{cases} \quad (14)$$

(4) New heat exchanger unit generation

Generating a new heat exchanger unit involves randomly selecting nodes from the hot and cold streams. In cases where no matching relationship exists between the selected nodes, a certain probability  $\theta$  is used to generate one new heat exchanger unit. The new unit is then assigned a random heat load. The implementation method is as follows:

$$Q_{H,\text{new}} = \begin{cases} Q_{\max} \times \omega_2 & , \text{ if } (r_2 < \theta) \\ 0 & , \text{ otherwise} \end{cases} \quad (15)$$

$$M_{H,\text{new}} = \begin{cases} N_{bH} \times \omega_3 & , \text{ if } (r_2 < \theta) \\ 0 & , \text{ otherwise} \end{cases} \quad (16)$$

$$M_{C,\text{new}} = \begin{cases} N_{bC} \times \omega_4 & , \text{ if } (r_2 < \theta) \\ 0 & , \text{ otherwise} \end{cases} \quad (17)$$

where  $Q_{\max}$  denotes the maximum heat load of the newly generated heat exchanger unit, and  $\omega_2$ ,  $\omega_3$ ,  $\omega_4$ , and  $r_2$  are random numbers between (0, 1).

(5) Selection and mutation operations

If the TAC of the evolved structure decreases compared to the previous iteration, it is accepted as the initial structure for the next iteration without any condition. However, if the TAC increases after evolution, the network with a higher cost is still considered with a certain probability, denoted as  $\delta$ . To decide whether to accept the imperfect solution with increased cost, a randomly generated number denoted as  $r_3$  is compared to  $\delta$ . If  $r_3$  is smaller

than  $\delta$ , the imperfect solution with the increased TAC is accepted as the initial structure for the next evolution iteration. Otherwise, the original structure from the previous iteration is retained.  $(f_n)_{it}$  represents the TAC of the HEN for the iteration numbered  $it$ , and  $(f_n)_{it+1}$  represents the TAC of the HEN for the  $(it + 1)$  iteration. The implementation method can be expressed as follows:

$$(f_n)_{it+1} = \begin{cases} (f_n'')_{it+1}, & \text{if } (f_n'')_{it+1} \leq (f_n)_{it} \\ (f_n'')_{it+1}, & \text{else if } (r_3 < \delta) \\ (f_n)_{it}, & \text{otherwise} \end{cases} \quad (18)$$

#### (6) Iteration termination

The calculation terminates when the iteration number reaches the maximum iteration  $IT_{\max}$ .

### 3.2. Infeasible Matching Caused by RWCE

Two common instances of impossible matching can arise when using heat loads of heat exchanger units as optimization variables in the NSM. One such instance is when a heat exchanger unit exhibits temperature crossover, and the other is when heat is transmitted from hot streams with lower temperatures to cold streams with higher temperatures. These infeasible matching structures can be handled through inner utilities or penalty methods, but they often come with an associated cost increase or penalty. The penalty or inner utilities substituting method in the NSM can lead to high penalty costs for these infeasible structures. As a result, most of these structures are typically not accepted during the optimization process, which can lead to wasted time at that particular iteration. Furthermore, the RWCE algorithm adopts a mechanism of accepting imperfect solutions. It accepts a small portion of these infeasible structures by allowing imperfect solutions. This approach may waste iteration steps and alter the optimization path.

#### 3.2.1. Temperature Crossover

Counter-current heat transfer is a widely employed method to enhance the heat transfer efficiency between cold and hot streams. However, a temperature crossover arises when the hot stream exhibits lower inlet and outlet temperatures than the cold stream, contradicting thermodynamic principles. This temperature crossover phenomenon can occur at the following heat exchanger location, as illustrated in Figure 3. The RWCE algorithm, commonly utilized for optimizing HENs, may accept imperfect structures with temperature crossovers due to its acceptance of imperfect solutions. Infeasible configurations are usually managed using the inner utilities substituting method or penalty functions to ensure the optimization process can continue. Unfortunately, the penalty method approach incurs additional costs, adversely affecting the optimization process and reducing overall efficiency.

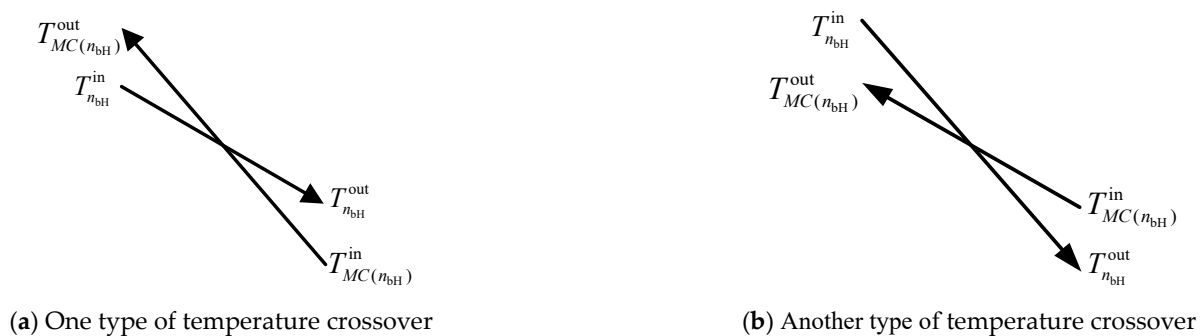
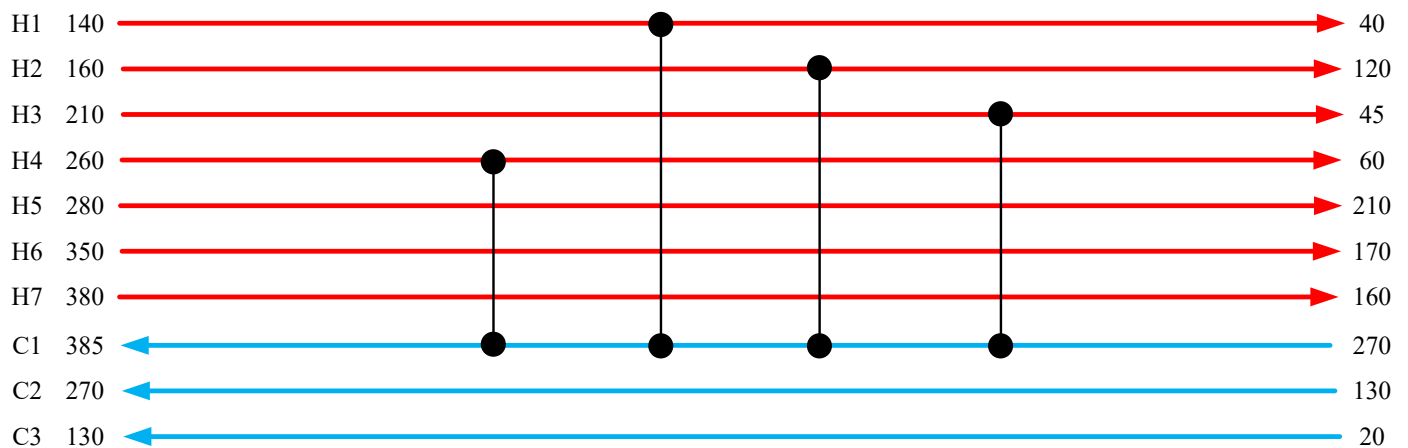


Figure 3. Schematic diagram of temperature crossover.

### 3.2.2. Extreme Match

The fundamental law of thermodynamics dictates that heat naturally flows from high-temperature objects to low-temperature objects, but not in the reverse direction. When the random pairing of nodes results in a hot node having a lower temperature than a cold node, heat transfer cannot occur, rendering the node pairing invalid. In the H7C3 case study [28], as shown in Figure 4, it is evident that the temperature level of the H1, H2, H3, and H4 streams is lower than that of the C1 stream. As a result, the heat exchanger pairings with their respective nodes are ineffective matches, leading to increased costs and rendering the configuration impractical.



**Figure 4.** H7C3 case with infeasible matching. “H”/“C” means the symbols of hot/cold streams; red and blue arrows represent the hot and cold streams, respectively. The value at the initial and final points of the arrows indicate the streams’ supply/target temperatures. A Black line and a set of bullets mean a heat exchanger unit, and the same as following figures.

### 3.2.3. Adverse Effects of Infeasible Structures

The typical approach of substituting with internal utilities or applying high-cost penalty functions is often used to address the infeasible structures generated during the HEN optimization. However, this approach can impact the optimization path and reduce the overall efficiency of the optimization process.

#### (1) Impact on optimization paths

The penalty function method is commonly employed to handle inequality constraints in optimization problems. It involves assigning a specific penalty value to infeasible solutions that violate the established rules. This penalty value increases the TAC associated with the infeasible solution, making it less favorable and, thus, less likely to be selected by the optimization algorithm during the selection mechanism. On the other hand, the selection mechanism of the RWCE algorithm incorporates the acceptance of imperfect solutions. It allows for accepting results with larger TAC values with a certain probability. The selection of imperfect solutions is determined randomly based on this probability, and as a result, some infeasible solutions can be included in the selection process under the RWCE algorithm. To illustrate this difference in approach, the H4C5 case [29] can be used as an example.

Accepting the infeasible solution at step 12,581,610 is a representative case illustrating its effect on the optimization path. In Figure 5, which demonstrates the change in cost during the optimization process of the nine-stream case, the point denoted as P represents the infeasible solution containing the penalty value accepted at step 12,581,610. As evident in Figure 5, the infeasible solution’s acceptance significantly impacts the TAC. Due to the penalty value associated with the infeasible solution, its TAC increases abruptly after being accepted. However, introducing this infeasible solution also obstructs the optimization

process of the original feasible solutions. The subsequent optimization paths evolve with this infeasible solution as the starting point, influencing the direction of the optimization. Consequently, some feasible solutions with evolutionary potential lose the opportunity to continue their evolution and may miss out on discovering better solutions. This effect leads to a decline in the optimization path and a stagnation in TAC, negatively impacting the overall optimization process.

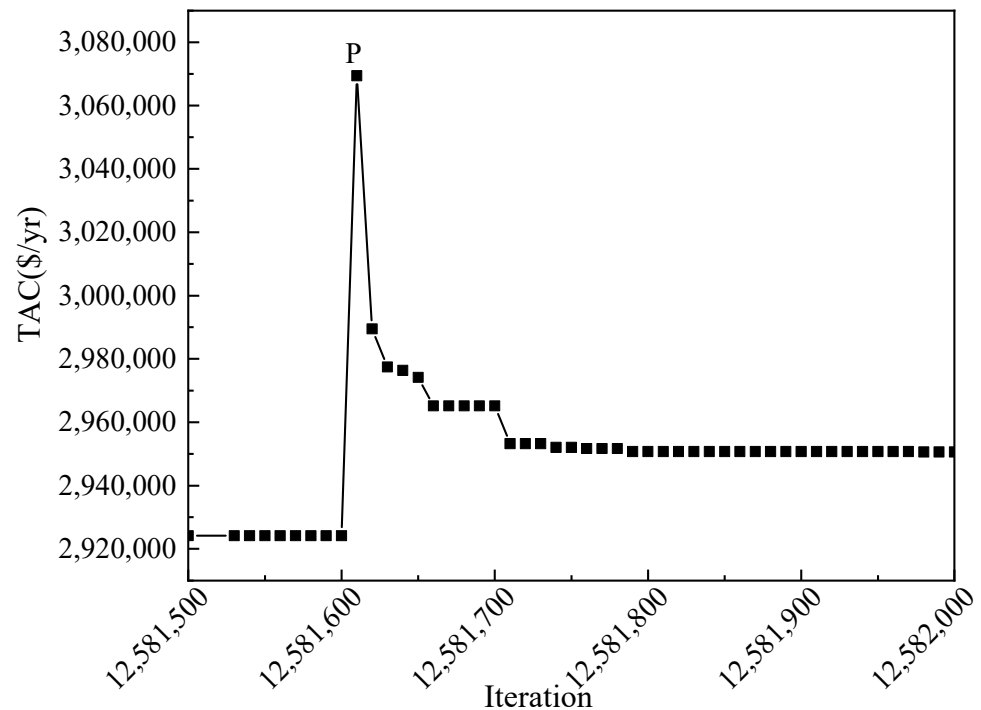


**Figure 5.** Variation of TAC for individual optimization process that accepts infeasible solutions.

## (2) Impact on optimization efficiency

Optimizing infeasible structures can lead to the rejection of most structures due to their high cost, resulting in wasted iteration time. While a small portion of infeasible structures is accepted by the imperfect acceptance mechanism of the RWCE algorithm, using such structures as initial configurations for the next iteration can waste additional iteration steps.

For example, in the H7C3 case depicted in Figure 6, assuming five nodes per stream and generating only one heat exchanger at a time, there are a total of  $7 \times 3 \times 5 = 525$  stream matching methods for node selection. Among these, when H1, H2, H3, and H4 are matched with the C1 stream, the resulting structure is invalid due to the mismatch of the hot stream's low-temperature portion with the cold stream's the high-temperature portion. A total of  $4 \times 5 \times 5 = 100$  combinations are produced with this invalid structure, accounting for 19% of the total matching methods. The listed invalid nodes, in this case, include only the nodes where the hot stream's lower temperature interval and the cold stream's higher temperature interval coincide, excluding any invalid node matches caused by temperature crossovers. The proportion of invalid matching structures in the randomly selected node matching is one fifth of the total ratio, leading to a further increase in cost and wasting computational resources and efficiency.

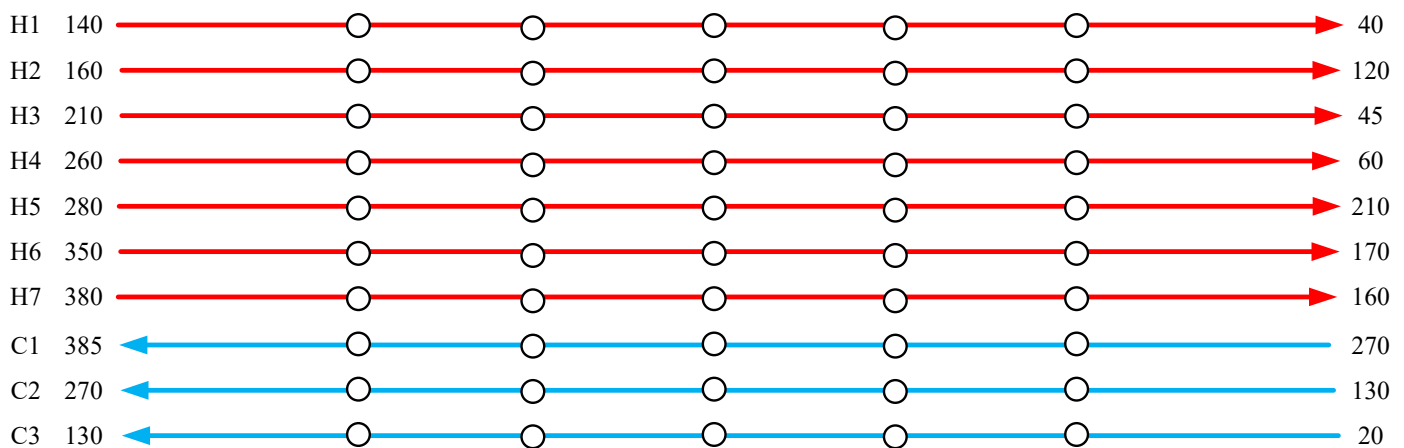


**Figure 6.** The NSM of the H7C3 case. The red and blue arrows represent the hot and cold streams, respectively. The hollow bullets represent the nodes on the hot and cold streams that can be selected to form heat exchanger units, and the same as following figures.

### 3.3. RWCE-TB Method

Based on the observed phenomenon of infeasible structures and their impact on optimization efficiency, accepting infeasible structures may lead to more iterations required to return to the feasible domain, making it challenging to find better structures and reducing optimization efficiency. Additionally, accepting infeasible structures, such as those with temperature crossovers or heat transfer from low-temperature to high-temperature sites, can replace the original, more feasible structures, further hindering the optimization process and affecting the optimization path. To address these issues, a new approach called the temperature interval tabu matching of RWCE (RWCE-TB) is proposed based on the rule of random matching of hot and cold nodes in the NSM.

#### 3.3.1. The RWCE-TB Method

The key idea of the RWCE-TB method is to prohibit the generation of invalid matched heat exchanger units, thus avoiding the adverse effects of infeasible structures on the entire HEN optimization process. The tabu conditions in RWCE-TB are divided into two categories. The first type of constraint occurs when an infeasible structure cannot be realized through inner utility substitutions. The second type of constraint arises when there is a mismatch in the heat exchanger unit, particularly when a low-temperature hot stream is matched with a high-temperature cold stream.

The primary process of the method is the same as that of the RWCE, except for a change in the operation of the new heat exchanger unit generation. A random empty node on the hot and cold streams is selected during the new individual generation stage to form a heat transfer match. If the temperature position meets the tabu-matching conditions, the location of the newly generated heat transfer unit is revisited to re-select the hot and cold streams. If not, the heat transfer match is randomly assigned a specific heat load, and a new heat transfer unit is generated, continuing the optimization downward. The stage of new heat exchanger generation of the RWCE is improved, as shown in Figure 7. The yellow parts are improvement to RWCE, while the blue one is the original parts of RWCE.

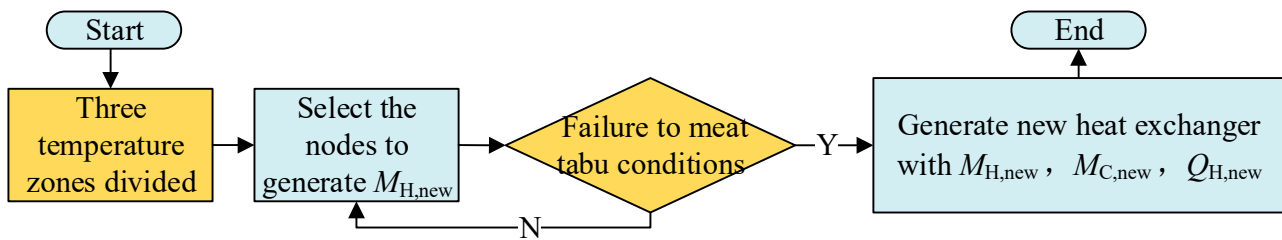


Figure 7. The flow chart of the new heat exchanger generation in RWCE-TB.

### 3.3.2. Steps of RWCE-TB Method

The main steps of the RWCE-TB method are as follows:

Step 1: Sort the temperatures

The import and export temperatures of all the hot and cold streams are sorted from smallest to largest and labeled sequentially to form an array, with the maximum value of the number being  $NT$ .

$$NT = 2(NH + NC) \quad (19)$$

Step 2: Divide the temperature intervals

Two temperatures,  $T_{low-mid}$  and  $T_{mid-high}$ , are defined as temperature boundaries to divide each stream of the HEN into three intervals: high temperature, medium temperature, and low temperature.  $T_{low-mid}$  is the boundary for the division of low to medium temperatures, and  $T_{mid-high}$  is the boundary for the division of medium to high temperatures. The two temperature boundaries are set as follows:

$$T_{low-mid} = T_{int(NT/3)+1} \quad (20)$$

$$T_{mid-high} = T_{int(2NT/3)+1} \quad (21)$$

where “int” is the round operator.

Step 3: Set the number of nodes

The allocation of nodes is based on the temperature intervals in which each stream is located and takes into account the maximum number of nodes allowed for a stream, denoted as  $N_{max}$ . Depending on the number of temperature intervals a stream spans, the nodes are allocated according to specific principles. Specifically, the number of nodes allocated for streams in only one temperature interval is denoted as  $N_1$ . For streams spanning two temperature intervals, the number of nodes assigned is denoted as  $N_2$ . Similarly, for streams spanning three temperature intervals, the number of nodes allocated is represented as  $N_3$ . The calculation of the number of nodes assigned for these three cases is determined using Equations (22)–(24).

$$N_1 = int(N_{max}/3) + 1 \quad (22)$$

$$N_2 = int(2 \cdot N_{max}/3) + 1 \quad (23)$$

$$N_3 = N_{max} \quad (24)$$

Step 4: Tabu match with temperature interval

When the RWCE algorithm enters the generation of the heat exchanger unit operation, it randomly selects a group of nodes to be excluded from forming a match under the following conditions:

Step 4.1: If the temperature level of the hot node is lower than the temperature level of the cold stream, as shown in Equation (25), the node is reselected.

$$T_{n_{bH}}^{\text{in}} < T_{MC(n_{bH})}^{\text{in}} \quad (25)$$

Step 4.2: If there is a temperature crossover between the hot and cold streams, as shown in Equations (26) and (27), the inner utilities substitute the infeasible stream matches. The heat load remains the same as the original amount at these nodes, as shown in Equation (28).

$$\begin{cases} T_{n_{bH}}^{\text{in}} - T_{MC(n_{bH})}^{\text{out}} < \Delta T_{\text{min}} \\ T_{n_{bH}}^{\text{out}} - T_{MC(n_{bH})}^{\text{in}} > \Delta T_{\text{min}} \end{cases} \quad (26)$$

$$\begin{cases} T_{n_{bH}}^{\text{in}} - T_{MC(n_{bH})}^{\text{out}} > \Delta T_{\text{min}} \\ T_{n_{bH}}^{\text{out}} - T_{MC(n_{bH})}^{\text{in}} < \Delta T_{\text{min}} \end{cases} \quad (27)$$

$$Q_{\text{incu},n_{bH}} = Q_{\text{inhu},MC(n_{bH})} = Q_{n_{bH}} \quad (28)$$

The hot stream exchanges heat with the inner cold utility. In contrast, the cold stream exchanges heat with the inner hot utility. In this case, the temperature can be obtained from Equations (29) and (30). If the constraint of the inner utilities is not met, as shown in Equations (31)–(34), the nodes are reselected.

$$LMTD_{n_{bH}}^{\text{inner}} = \begin{cases} \frac{(T_{n_{bH}}^{\text{in}} - T_{CU}^{\text{out}}) - (T_{n_{bH}}^{\text{out}} - T_{CU}^{\text{in}})}{\ln\left(\frac{T_{n_{bH}}^{\text{in}} - T_{CU}^{\text{out}}}{T_{n_{bH}}^{\text{out}} - T_{CU}^{\text{in}}}\right)}, T_{n_{bH}}^{\text{in}} - T_{CU}^{\text{out}} \neq T_{n_{bH}}^{\text{out}} - T_{CU}^{\text{in}} \\ \frac{(T_{n_{bH}}^{\text{in}} - T_{CU}^{\text{out}}) + (T_{n_{bH}}^{\text{out}} - T_{CU}^{\text{in}})}{2}, T_{n_{bH}}^{\text{in}} - T_{CU}^{\text{out}} = T_{n_{bH}}^{\text{out}} - T_{CU}^{\text{in}} \end{cases} \quad (29)$$

$$LMTD_{MC(n_{bH})}^{\text{inner}} = \begin{cases} \frac{(T_{HU}^{\text{in}} - T_{MC(n_{bH})}^{\text{out}}) - (T_{HU}^{\text{out}} - T_{MC(n_{bH})}^{\text{in}})}{\ln\left(\frac{T_{HU}^{\text{in}} - T_{MC(n_{bH})}^{\text{out}}}{T_{HU}^{\text{out}} - T_{MC(n_{bH})}^{\text{in}}}\right)}, T_{HU}^{\text{in}} - T_{MC(n_{bH})}^{\text{out}} \neq T_{HU}^{\text{out}} - T_{MC(n_{bH})}^{\text{in}} \\ \frac{(T_{HU}^{\text{in}} - T_{MC(n_{bH})}^{\text{out}}) + (T_{HU}^{\text{out}} - T_{MC(n_{bH})}^{\text{in}})}{2}, T_{HU}^{\text{in}} - T_{MC(n_{bH})}^{\text{out}} = T_{HU}^{\text{out}} - T_{MC(n_{bH})}^{\text{in}} \end{cases} \quad (30)$$

$$T_{n_{bH}}^{\text{in}} - T_{CU}^{\text{out}} > 0.0 \quad (31)$$

$$T_{n_{bH}}^{\text{out}} - T_{CU}^{\text{in}} > 0.0 \quad (32)$$

$$T_{HU}^{\text{in}} - T_{MC(n_{bH})}^{\text{out}} > 0.0 \quad (33)$$

$$T_{HU}^{\text{out}} - T_{MC(n_{bH})}^{\text{in}} > 0.0 \quad (34)$$

where  $LMTD_{n_{bH}}^{\text{inner}}$  and  $LMTD_{MC(n_{bH})}^{\text{inner}}$  are the logarithmic mean temperature difference at the hot node  $n_{bH}$  and cold node  $MC(n_{bH})$ , respectively.

#### 4. Cases Analysis

This section will implement and demonstrate the proposed heuristic algorithm with tabu matching to solve three classical HEN cases: H6C4, H7C3, and H13C7. We will compare the results obtained from our algorithm with the results reported in the literature for other methods to showcase the global search capability of our proposed method. The parameters of the RWCE algorithm and the number of nodes in the NSM are set as specified in Table 1.

**Table 1.** Parameter settings for calculation of the three cases.

	$N$	$\Delta L$	$Q_{\max}$	$Q_{\min}$	$\tau$	$\theta$	$\delta$	$N_{\max}$	$IT_{\max}$
H6C4	10	100	200	5	0.2	0.2	0.01	14	$8 \times 10^8$
H7C3	30	200	850	5	0.2	0.2	0.005	30	$8 \times 10^8$
H13C7	30	80	120	10	0.2	0.2	0.01	9	$8 \times 10^8$

#### 4.1. Case 1 (H6C4)

Case 1 comprises ten streams, with six hot streams and four cold streams. The stream parameters are listed in Table 2. This example focuses on a typical test case, which has been extensively investigated by researchers to evaluate the performance of algorithms [28]. In this regard, Ahmad [28] utilized the pinch point method to achieve a minimum TAC of USD 707,400/yr. Yerramsetty [30] used a differential evolution method for simultaneous optimization and obtained a minimum TAC of USD 5,666,765/yr. Khorasany [31] proposed a hybrid optimization method and achieved a minimum TAC of USD 5,662,366/yr for this case. Zhang [32] employed an efficient process stream arrangement strategy based on a chessboard representation, resulting in a minimum TAC of USD 5,607,762/yr. Rathjens et al. [33] proposed a local optimization method embedded in a stochastic global search with a customized genetic algorithm and an SWS model. Xu et al. [34] introduced a phased modular concept, supporting functional and sub-functional combinations for efficient optimization. Chen et al. [35] proposed a polymorphic firefly algorithm with a self-adaptation method and achieved a minimum TAC of USD 5,592,255/yr.

**Table 2.** Problem data and annual costs of heat exchanger units of case study 1.

Stream	$T^{\text{in}}$ (°C)	$T^{\text{out}}$ (°C)	$F_{\text{Cp}}$ (kW/°C)	$h$ (kW/(m·°C))
H1	85	45	156.3	0.05
H2	120	40	50.0	0.05
H3	125	35	23.9	0.05
H4	56	46	1250	0.05
H5	90	86	1500	0.05
H6	225	75	50	0.05
C1	40	55	466.7	0.05
C2	55	65	600	0.05
C3	65	165	180	0.05
C4	10	170	81.3	0.05
HU	200	198	-	0.05
CU	15	20	-	0.05

Annual cost of heat exchanger = 60 A (USD/yr) (A in m<sup>2</sup>)

Annual cost of hot utility = USD 100/kW/yr

Annual cost of cold utility = USD 15/kW/yr

The RWCE with the tabu-matching temperature intervals strategy is applied to optimize the HEN, determining temperature boundaries of 56 °C for the medium and low-temperature level intervals and 86 °C for the medium and high-temperature level intervals. The streams across three temperature level intervals, H2, H3, and C4, are each assigned nine nodes. The streams across two temperature level intervals, including H1, H6, C2, and C3, are allocated six nodes each. Lastly, the streams across one temperature level interval, H4, H5, and C1, are assigned three nodes each, as illustrated in Figure 8. The results of the HEN optimization using the NSM model with the original RWCE method (NSM & RWCE) and the RWCE with tabu-matching method (NSM & RWCE-TB) are shown in Figures 9 and 10. Moreover, a comparison with published results is presented in Table 3.



**Table 3.** Comparison of optimization results for case 1.

Literature	Units	Hot Utility/MW	Cold Utility/MW	TAC/USD/yr
Ahmad [28]	-	15,400	9796	7,074,000
Yerramstetty et al. [30]	13	20,754	15,140	5,666,756
Khorasany [31]	12	19,605	14,000	5,662,366
Zhang et al. [32]	19	20,276	14,670	5,607,762
Peng and Cui [14]	18	20,339	14,733	5,596,079
Rathjens et al. [33]	12	20,420	14,815	5,713,267
Xu et al. [34]	13	20,377	14,795	5,704,465 (with splits)
Chen [35]	19	20,540	14,935	5,592,255
NSM&RWCE (Figure 9)	22	20,250	14,644	5,589,808
NSM&RWCE-TB (Figure 10)	21	20,308	14,703	5,588,154

Different colors represent various temperature intervals where each node is located, with red indicating the high-temperature interval, yellow for the medium-temperature interval, and blue for the low-temperature interval. The absence of a heat exchanger with a blue solid circle on the hot stream and a red solid circle on the cold stream indicates that the low-temperature level of the hot stream cannot be matched with the high-temperature level of the cold stream. Furthermore, neither figure has temperature crossover matching, indicating that such configurations are not allowed in the free-matching temperature intervals. However, the random matching in the NSM & RWCE method may produce heat exchanger units with matches on H4, C2, and C3, which are infeasible connections. The optimization process requires multiple iteration steps to eliminate these invalid matching structures. In contrast, the proposed method reduces the need for iterations to eliminate such invalid matches within the same number of iteration steps. As a result, it achieves a cost reduction of USD 1465/yr compared to the original NSM & RWCE approach at the same maximum iteration. Additionally, the proposed method performs better when compared with the literature results and achieves a cost reduction of USD 4101/yr compared to the literature results [20]. The results exhibit a decrease of 21% in comparison to the outcomes presented by Ahmad [28]. These findings highlight the efficacy of the methodology presented in this paper.

#### 4.2. Case 2 (H7C3)

Case 2 consists of seven hot and three cold streams, first presented by Ahmad in the literature [36]. Table 4 provides problem data and the annual costs of heat exchanger units (Table 4). Ahmad obtained the minimum TAC using the pinch point method, which was USD 9,490,000/yr. Liu et al. [37] used a hybrid genetic algorithm and achieved a minimum annual integrated cost of USD 8,917,245/yr for the final structure of this case. Additionally, Liu et al. [38] used the RWCE algorithm with an improved step size to optimize the SWS model and obtained a minimum annual integrated cost of USD 8,707,983/yr for this example. The proposed method exhibits better performance compared to the literature results (Table 5) in this paper.

The division of temperature intervals and node assignments for Case 2 is shown in Figure 11. The results obtained using the NSM & RWCE and NSM & RWCE-TB methods are depicted in Figures 12 and 13, respectively. One significant difference between the two structures is the varying number of heat exchanger units in the network. Since the fixed investment cost is not considered in this example, the presence of more heat exchanger units in the proposed method does not incur additional fixed investment costs. As a result, the proposed method includes seven more heat transfer units than the original model. The TAC of the proposed method is lower than that of the NSM & RWCE method because it obtains less utility heat transfer, leading to a reduction in the TAC.

**Table 4.** Problem data and annual costs of heat exchanger units of case study 2.

Stream	$T^{in}$ (°C)	$T^{out}$ (°C)	$F_{Cp}$ (kW/°C)	$h$ (kW/(m <sup>2</sup> ·°C))
H1	140.0	40.0	470.0	0.8
H2	160.0	120.0	825.0	0.8
H3	210.0	45.0	42.4	0.8
H4	260.0	60.0	100.0	0.8
H5	280.0	210.0	357.1	0.8
H6	350.0	170.0	50.0	0.8
H7	380.0	160.0	136.4	0.8
C1	270.0	385.0	826.1	0.8
C2	130.0	270.0	500.0	0.8
C3	20.0	130.0	363.6	0.8
HU	500	499	-	0.8
CU	20	40	-	0.8

Annual cost of heat exchanger = 300 A (USD/yr) (A in m<sup>2</sup>)  
 Annual cost of hot utility = USD 60/kW/yr  
 Annual cost of cold utility = USD 5/kW/yr

**Table 5.** Comparison of optimization results for case 2.

Literature	Units	Hot Utility/MW	Cold Utility/MW	TAC/USD/yr
Ahmad [36]	11	-	-	9,490,000
Liu et al. [37]	15	92.93	58.93	8,917,245
Liu et al. [38]	31	92.40	58.40	8,707,983
NSM & RWCE (Figure 12)	27	92.68	58.68	8,715,491
NSM & RWCE-TB (Figure 13)	33	92.42	58.42	8,706,548

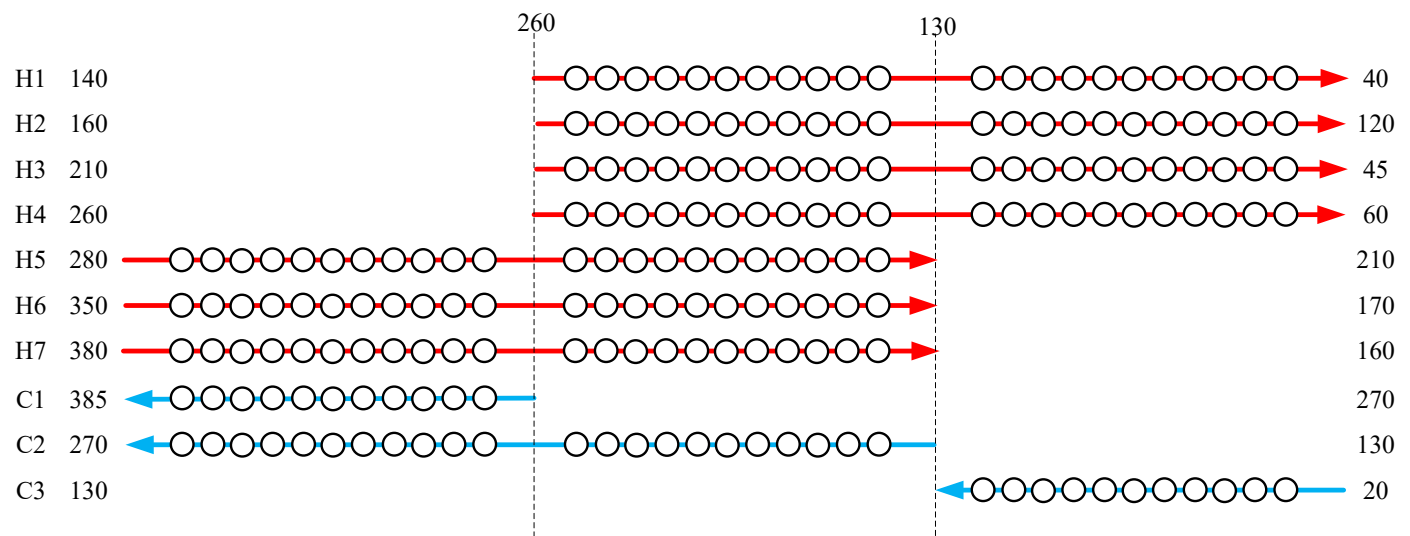


**Figure 11.** Division of temperature intervals and node assignment for case 2.

The two structures obtained using NSM & RWCE and NSM & RWCE-TB methods share some similarities. Both structures have no heat exchanger on the H1 stream and only one cold utility. Additionally, there are more heat exchanger units on C2, and no heat exchanger units are present between the hot streams H1, H2, H3, and H4 and the cold stream C1 in the final structure of both HENs. However, the optimization process of the NSM & RWCE method requires several iterations to eliminate the heat exchange units between H1, H2, H3, and H4 and the cold stream C1 to achieve a better structure. On the other hand, the temperature-based tabu-matching heuristic method in NSM & RWCE-TB restricts the generation of such infeasible heat exchanger units, improving the optimization

quality of the HEN. As a result, the minimum TAC obtained from the NSM & RWCE-TB method is USD 8943/yr lower than that of the NSM & RWCE method, and USD 1435/yr lower than the best reported in the literature by Liu et al. [38].

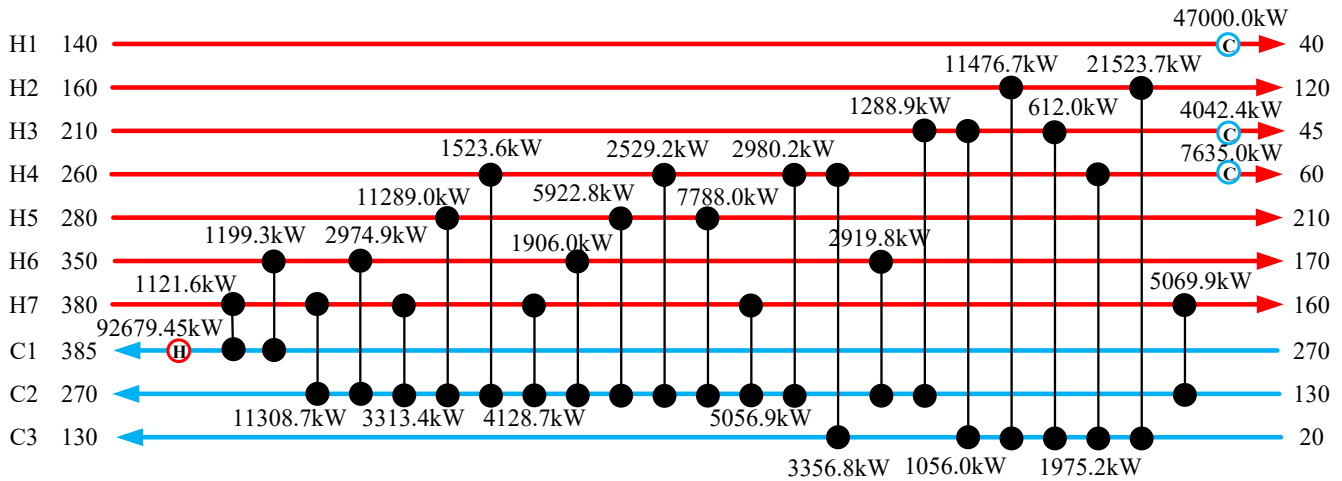


Figure 12. Optimization results of the NSM & RWCE method (TAC= USD 8,715,496/yr).

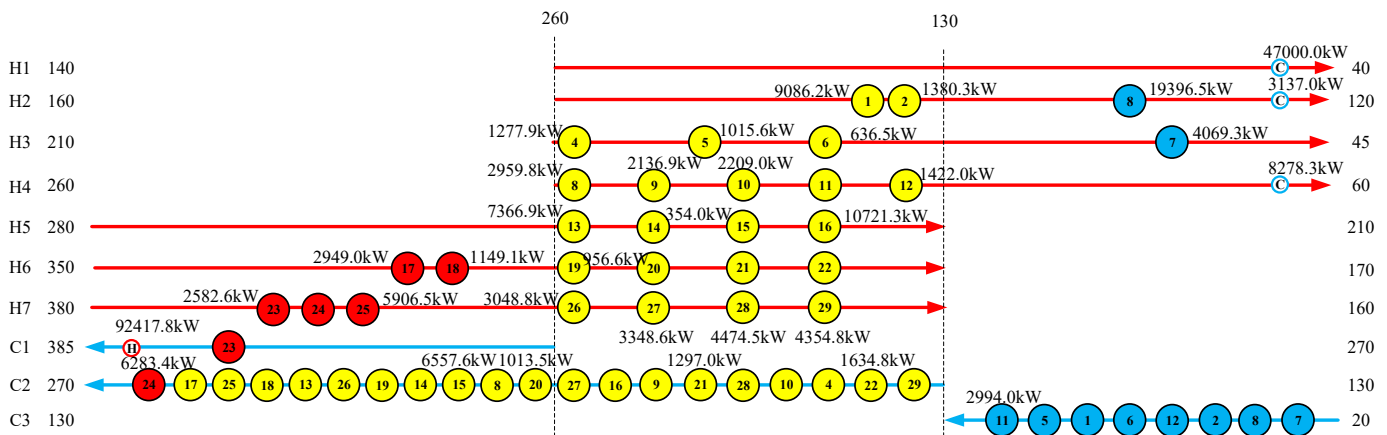


Figure 13. Optimization results of the NSM&RWCE-TB method (TAC = USD 8,706,548/yr).

### 4.3. Case 3 (H13C7)

Case three consists of thirteen hot and seven cold streams, initially proposed by Kravanja and Soršak [39]. The specific parameters of the example are listed in Table 6. Several studies have previously optimized this case using different algorithms and obtained various minimum TAC values. For instance, Pavão et al. [40] used a combination of genetic and particle swarm algorithms to achieve a minimum TAC of USD 1,516,482/yr. Xiao et al. [41] optimized an SWS model and RWCE with a fine search strategy to obtain a minimum TAC of USD 1,447,482/yr. Zhang et al. [42] used a modified cuckoo algorithm and achieved a minimal TAC of USD 1,418,981/yr. Xu et al. [43] proposed a relaxation strategy for HEN synthesis with non-zero fixed capital costs. The generation and elimination of heat exchangers are promoted by retrofitting the formulation of costs, leading to a TAC of USD 1,412,801/yr. Caballero et al. [44] proposed a sequential approach combining the TransHEN and the HENDesign model, obtaining a TAC of USD 1,414,831/yr. Chang et al. [45] developed a global optimum search algorithm with a TAC of USD 1,407,203/yr.

For this case, the temperature boundaries for the low and medium temperature intervals are set at 140 °C, while those for the high and medium temperature intervals are set at 322 °C. The streams H1, H2, H3, H6, H7, H9, H10, H11, H12, H13, C3, C5, C6, and C7 spanning one temperature interval are assigned three nodes thereon, the streams H4,

H5, C2, and C4 spanning two temperature intervals are posted with six nodes, and nine nodes are given to the stream C1 spanning three temperature level intervals, as shown in Figure 14. The configurations are shown in Figures 15 and 16.

**Table 6.** Problem data and annual costs of heat exchanger units of case study 3.

Stream	$T^{\text{in}}$ (°C)	$T^{\text{out}}$ (°C)	$F_{\text{Cp}}$ (kW/°C)	$h$ (kW/(m <sup>2</sup> ·°C))
H1	576	437	23.1	0.06
H2	599	399	15.22	0.06
H3	530	382	15.15	0.06
H4	449	237	14.76	0.06
H5	368	177	10.7	0.06
H6	121	114	149.6	1.0
H7	202	185	258.2	1.0
H8	185	113	8.38	1.0
H9	140	120	59.89	1.0
H10	69	66	165.79	1.0
H11	120	68	8.74	1.0
H12	67	35	7.62	1.0
H13	1034.5	576	21.3	0.06
C1	123	343	10.61	0.06
C2	20	156	6.65	1.2
C3	156	157	3291	2.0
C4	20	182	26.63	1.2
C5	182	318	31.19	1.2
C6	318	320	4011.83	2.0
C7	322	923.78	17.6	0.06
HU	927	927	-	5.0
CU	9	17	-	1.0

Annual cost of heat exchanger =  $4000 + 500 A^{0.83}$  (USD/yr) (A in m<sup>2</sup>)  
 Annual cost of hot utility = USD 250/kW/yr  
 Annual cost of cold utility = USD 25/kW/yr

In both Figures 15 and 16, all heat exchanger units are matched by stream nodes in adjacent or the same temperature intervals. The NSM & RWCE method resulted in four utilities, while the NSM & RWCE-TB method yielded three. The total number of possible matching relationships between hot and cold stream nodes in the optimization process is reduced despite the temperature interval tabu-matching strategy limiting infeasible matches. However, this does not impact the diversity of individual evolutions in the feasible domain, leading to high-quality optimization results. Table 7 indicates that the results presented in this paper are generally superior to those reported in previous publications. Comparing the proposed methodology to the original NSM-RWCE algorithm, it is found that the former leads to an annual savings of USD 5430. Moreover, it outperforms the literature findings [45] by 0.80%.

**Table 7.** Comparison of optimization results for case 3.

Literature	Units	Hot Utility/MW	Cold Utility/MW	TAC/USD/yr
Pavão et al. [40]	21	1938	106.93	1,516,482 (with splits)
Xiao et al. [41]	23	1.868	36.6	1,447,482
Zhang et al. [42]	22	1.831	0.00	1,418,981
Xu et al. [43]	21	1.831	0.04	1,412,801
Caballero et al. [44]	21	1.831	0.00	1,414,831 (with splits)
Chang [45]	20	1.831	0.00	1,407,203 (with splits)
NSM & RWCE (Figure 15)	22	1.831	0.00	1,401,311
NSM & RWCE-TB (Figure 16)	21	1.831	0.00	1,395,971

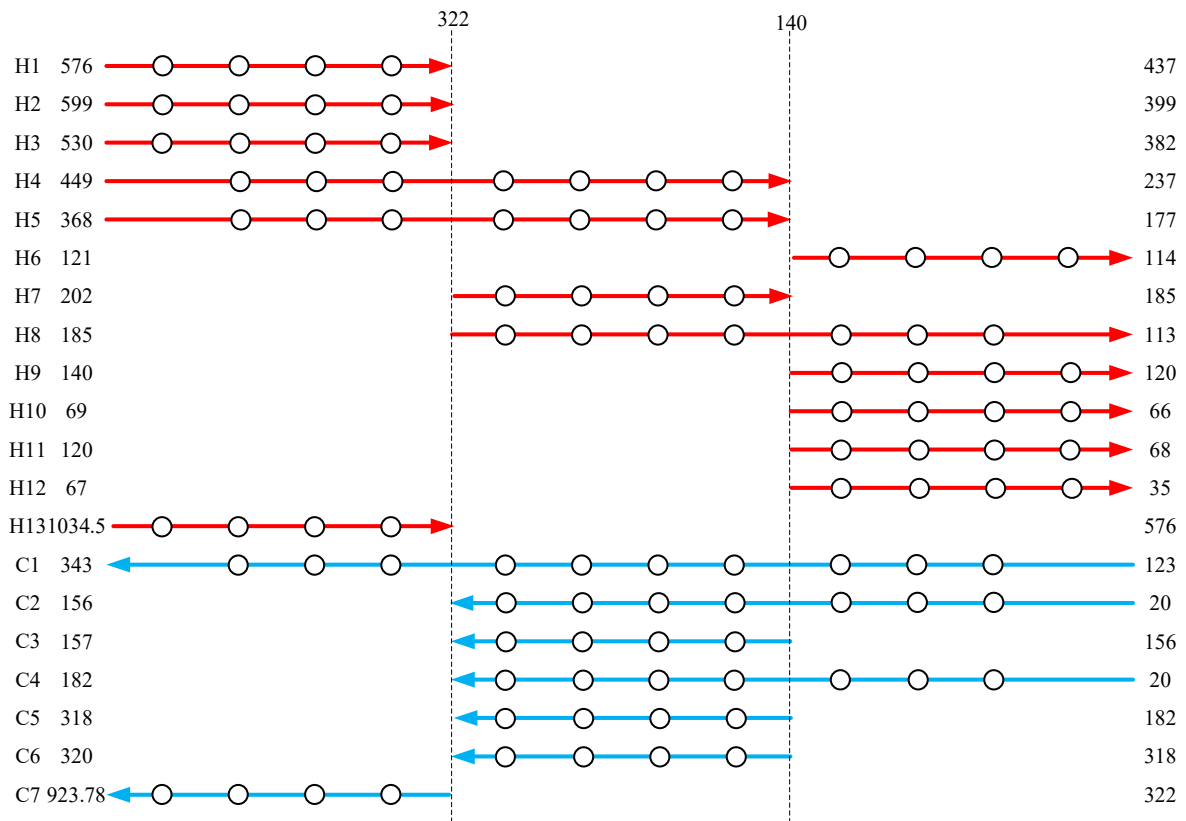


Figure 14. Division of temperature intervals and node assignment for case 3.

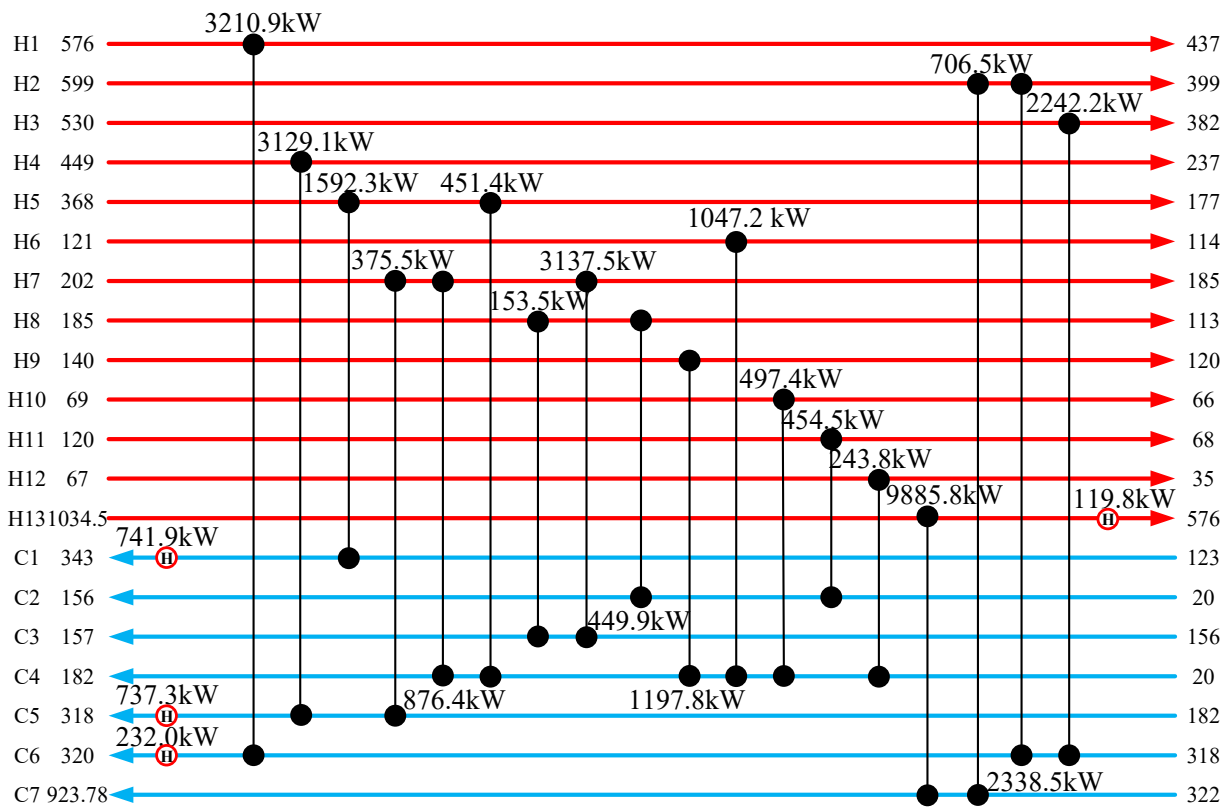


Figure 15. Optimization results of the NSM & RWCE method (TAC= USD 1,401,311/yr).

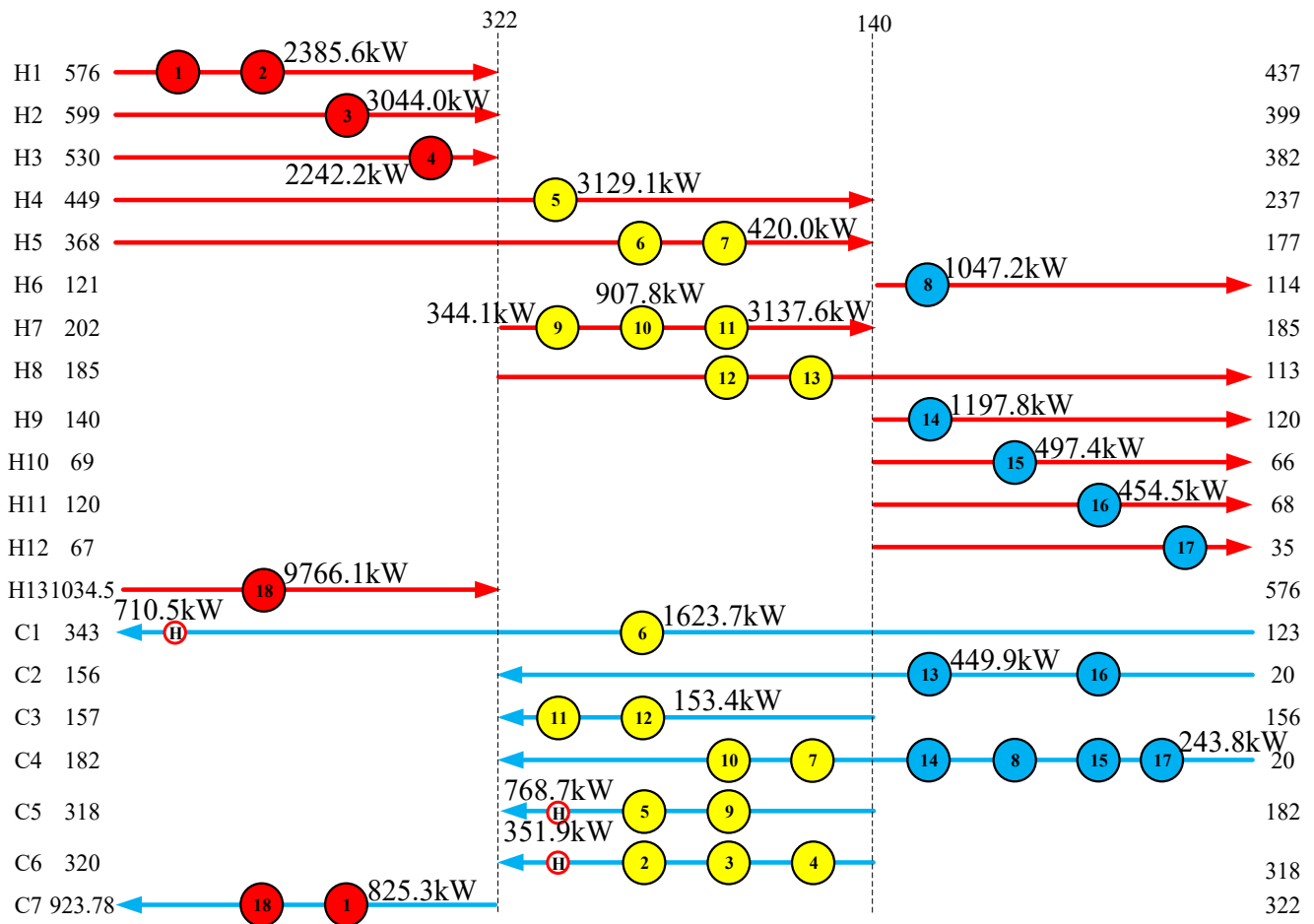


Figure 16. Optimization results of the NSM & RWCE-TB method (TAC = USD 1,395,971/yr).

4.4. Algorithm Efficiency Analysis

The computational times of three cases are presented in Table 8 to illustrate the search capabilities of the RWCE-TB algorithm. It should be indicated that computations were carried out on a Windows Server system comprising an Intel(R) Core (TM) i5-7200 U CPU @ 2.50 GHz 2.70 GHz. The programming was executed in a Compaq Visual Fortran Version 6.6 platform.

Table 8. The computational times for three test cases.

Case	Computational Time (s) of the NSM & RWCE	Computational Time (s) of the NSM & RWCE-TB	Efficiency Improvement (%)
case1	10,585	8891	16.0%
case2	13,311	9158	31.2%
case3	64,619	50,209	22.3%

Table 8 indicates that the efficiency of the NSM & RWCE-TB algorithm outperforms that of the traditional NSM & RWCE method in the studied cases. These results confirm that RWCE-TB boasts heightened search efficiency. Since simultaneous HEN synthesis is categorized as an NP-hard problem, solution accuracy within a reasonable computational timeframe takes precedence. Consequently, the TAC is utilized as the standard measure for evaluating solution efficacy. Due to various programming approaches and computation hardware, comparing computation times across different methods is challenging. Accordingly, comparing computation times can be achieved under standardized programming

conditions. Hence, this paper refrains from comparing computational efficiency with other methods. In optimizing complex systems, the primary focus of this article remains on the quality of global optimization outcomes.

## 5. Conclusions

This paper presents a heuristic algorithm with tabu matching for HEN synthesis, aiming to enhance the optimization quality of the heuristic optimization method. The method is refined upon the foundation of the RWCE algorithm. It initiates by introducing the concept of high-, medium-, and low-temperature intervals. Subsequently, the number of nodes is dynamically determined according to these temperature intervals. The nodes on streams are flexibly matched within the framework of tabu rules, which prevents the matching of the low-temperature interval of hot streams with the high-temperature interval of cold streams, as well as streams that occur at temperature crossing. The primary innovation of this method lies in its capacity to prevent matches between streams exhibiting infeasible structures grounded in thermodynamic principles. This innovation concurrently limits the production of infeasible solutions while maintaining the extent of the viable region. The performed analyses demonstrate that compared with published data, the obtained TACs for H6C4, H7C3, and H13C7 case studies decrease by USD 4290/yr, USD 1435/yr, and USD 11,232/yr, respectively. Furthermore, the comparison of computational times shows that the proposed RWCE-TB algorithm outperforms the conventional RWCE in terms of computational efficiency, with a maximum improvement in efficiency of 31.2%. In addition to its computational advantages, the proposed model is easy to implement and can be applied to other heuristic methods.

**Author Contributions:** Conceptualization, G.C.; data curation, X.H.; investigation, W.Y.; methodology, X.H.; resources, G.C.; software, X.H. and H.S.; validation, H.S.; visualization, W.Y.; writing—original draft, X.H.; writing—review and editing, H.D. All authors have read and agreed to the published version of the manuscript.

**Funding:** This research was funded by National Natural Science Foundation of China grand (Grant No. 21978171).

**Data Availability Statement:** Not applicable.

**Conflicts of Interest:** The authors declare no conflict of interest.

## Nomenclature

### Abbreviations

TAC	Total annual cost
HENS	Heat exchanger network synthesis
MINLP	Mixed-integer nonlinear programming
HEN	Heat exchanger network
SWS	Stage-wise superstructure
NSM	Non-structural model
RWCE	Random walk with compulsive evolution
RWCE-TB	Improved Random walk with compulsive evolution with temperature interval tabu matching

### Variables

$A$	Heat transfer area, $m^2$
$C_A$	Area cost coefficient of cold utility, heat exchangers, hot utility, USD/yr
$C_{CU}$	Utility cost coefficient of cold utility, USD/yr
$C_{HU}$	Utility cost coefficient of hot utility, USD/yr
$h$	Coefficient of convective heat transfer, $kw/m^2/^\circ C$
$Q$	Heat load, kw
$Q_{CU}$	Heat load of cold utility, kW
$Q_{HU}$	Heat load of hot utility, kW
$F_{Fix}$	Fixed charge of cold utility, heat exchangers, hot utility, USD/yr
$F_{Cp}$	Heat capacity flow rate, $kw/^\circ C$

$it$	Iteration step
$(f_n)_{it}$	TAC of individual $n$ at iteration $it$ , USD/yr
$IT_{\max}$	Maximum number of iterations
$N_P$	Population size
$N_H$	Number of hot streams
$N_C$	Number of cold streams
$N_{bH}$	Number of hot nodes
$N_{bC}$	Number of cold nodes
$\phi$	Evolution probability
$Q_{\min}$	Minimum threshold of heat load, kW
$Q_{\max}$	Maximum threshold of heat load, kW
$T$	Temperature, °C
$\delta$	Probability of accepting imperfect solutions
$\Delta L$	The maximum walk step of heat loads, kW
$\varepsilon$	Exponent for area cost
$\theta$	Generation probability
$n_{bH}$	Serial number of the hot stream node
$n_{bC}$	Serial number of the cold stream node
$LMTD$	Logarithmic mean temperature difference, °C
$MC(n_{bH})$	Serial number of the cold node connected with the hot stream node $n_{bH}$
$M_{H,new}$	Position of the newly generated hot node
$M_{C,new}$	Position of the newly generated cold node
$N_{\max}$	The maximum number of nodes of a stream
$X$	Variable is a binary variable with a value range of 0 and 1
$\Delta T_{\min}$	minimum approach temperature, °C
$N_{dH}$	number of node on each hot stream
$N_{dC}$	number of node on each cold stream
Superscripts	
in	Inlet of streams
out	Outlet of streams
inner	Inner utility
Subscripts	
C	Cold stream
CU	Cold utility
HU	Hot utility
H	Hot stream
$i$	Hot stream index
$j$	Cold stream index
$it$	Iteration index
min	Minimum
inhu	Inner hot utility
incu	Inner cold utility
new	New heat exchanger unit

## References

1. Amer, M.; Chen, M.-R.; Sajjad, U.; Ali, H.M.; Abbas, N.; Lu, M.-C.; Wang, C.-C. Experiments for suitability of plastic heat exchangers for dehumidification applications. *Appl. Therm. Eng.* **2019**, *158*, 654–664. [[CrossRef](#)]
2. Short, M.; Isafiade, A.J. Thirty years of mass exchanger network synthesis—A systematic review. *J. Clean. Prod.* **2021**, *304*, 127112. [[CrossRef](#)]
3. Chang, C.; Liao, Z.; Bagajewicz, M.J. New superstructure-based model for the globally optimal synthesis of refinery hydrogen networks. *J. Clean. Prod.* **2021**, *292*, 126022. [[CrossRef](#)]
4. Kamat, S.; Bandyopadhyay, S.; Foo, D.C.Y.; Liao, Z. State-of-the-art review of heat integrated water allocation network synthesis. *Comput. Chem. Eng.* **2022**, *167*, 108003. [[CrossRef](#)]
5. Lin, C.; Wang, B. Combined Heat and Power Dispatch with Start-Stop Schedule of Heat Exchange Stations. In Proceedings of the 2018 IEEE Power & Energy Society General Meeting (PESGM), Portland, OR, USA, 5–9 August 2018; pp. 1–5.
6. Yang, X.; Sun, Y.; Wu, W.; Liu, H.; Wang, Y. Coordinated real-time power dispatch for integrated transmission and distribution networks based on model-based optimization and deep reinforcement learning. *Energy Rep.* **2023**, *9*, 1011–1020. [[CrossRef](#)]

7. Zheng, W.; Lu, H.; Zhang, M.; Wu, Q.; Hou, Y.; Zhu, J. Distributed Energy Management of Multi-Entity Integrated Electricity and Heat Systems: A Review of Architectures, Optimization Algorithms, and Prospects. *IEEE Trans. Smart Grid* **2023**, *1*. [[CrossRef](#)]
8. Linnhoff, B.; Flower, J.R. Synthesis of heat exchanger networks: I. Systematic generation of energy optimal networks. *AIChE J.* **1978**, *4*, 633–642. [[CrossRef](#)]
9. Linnhoff, B.; Hindmarsh, E. The pinch design method for heat exchanger networks. *Chem. Eng. Sci.* **1983**, *38*, 745–763. [[CrossRef](#)]
10. Zamora, J.M.; Grossmann, I.E. A comprehensive global optimization approach for the synthesis of heat exchanger networks with no stream splits. *Comput. Chem. Eng.* **1997**, *21*, 65–70. [[CrossRef](#)]
11. Bergamini, M.L.; Grossmann, I.; Scenna, N.; Aguirre, P. An improved piecewise outer-approximation algorithm for the global optimization of MINLP models involving concave and bilinear terms. *Comput. Chem. Eng.* **2008**, *32*, 477–493. [[CrossRef](#)]
12. Lin, B.; Miller, D.C. Solving heat exchanger network synthesis problems with Tabu Search. *Comput. Chem. Eng.* **2004**, *28*, 1451–1464. [[CrossRef](#)]
13. Dipama, J.; Teysseidou, A.; Sorin, M. Synthesis of heat exchanger networks using genetic algorithms. *Appl. Therm. Eng.* **2008**, *28*, 1763–1773. [[CrossRef](#)]
14. Peng, F.; Cui, G. Efficient simultaneous synthesis for heat exchanger network with simulated annealing algorithm. *Appl. Therm. Eng.* **2015**, *78*, 136–149. [[CrossRef](#)]
15. Xiao, Y.; Cui, G. A novel Random Walk algorithm with Compulsive Evolution for heat exchanger network synthesis. *Appl. Therm. Eng.* **2017**, *115*, 1118–1127. [[CrossRef](#)]
16. Fu, D.; Yu, Z.; Lai, Y. Linking pinch analysis and shifted temperature driving force plot for analysis and retrofit of heat exchanger network. *J. Clean. Prod.* **2021**, *315*, 128235. [[CrossRef](#)]
17. Orosz, Á.; How, B.S.; Friedler, F. Multiple-solution heat exchanger network synthesis using P-HENS solver. *J. Taiwan Inst. Chem. Eng.* **2022**, *130*, 103859. [[CrossRef](#)]
18. Lakner, R.; Orosz, Á.; How, B.S.; Friedler, F. Synthesis of multiperiod heat exchanger networks: N-best networks with variable approach temperature. *Therm. Sci. Eng. Prog.* **2023**, *42*, 137696. [[CrossRef](#)]
19. Yee, T.F.; Grossman, I.E. Simultaneous optimization models for heat integration. II. Heat exchanger network synthesis. *Comput. Chem. Eng.* **1990**, *14*, 1165–1184. [[CrossRef](#)]
20. Pavão, L.V.; Costa, C.B.B.; Ravagnani, M.A.S.S. Heat exchanger networks retrofit with an extended superstructure model and a meta-heuristic solution approach. *Comput. Chem. Eng.* **2019**, *125*, 380–399. [[CrossRef](#)]
21. Pavão, L.V.; Costa, C.B.B.; Ravagnani, M.A.S.S. A new stage-wise superstructure for heat exchanger network synthesis considering substages, sub-splits and cross flows. *Appl. Therm. Eng.* **2018**, *143*, 719–735. [[CrossRef](#)]
22. Na, J.; Jung, J.; Park, C.; Han, C. Simultaneous synthesis of a heat exchanger network with multiple utilities using utility substages. *Comput. Chem. Eng.* **2015**, *79*, 70–79. [[CrossRef](#)]
23. Huang, Y.; Zhuang, Y.; Xing, Y.; Liu, L.; Du, J. Multi-objective optimization for work-integrated heat exchange network coupled with interstage multiple utilities. *Energy* **2023**, *273*, 127240. [[CrossRef](#)]
24. Xiao, Y.; Kayange, H.A.; Cui, G.; Chen, J. Non-structural model of heat exchanger network: Modeling and optimization. *Int. J. Heat Mass Transf.* **2019**, *140*, 752–766. [[CrossRef](#)]
25. Aguitoni, M.C.; Pavão, L.V.; da Silva Sá Ravagnani, M.A. Heat exchanger network synthesis combining Simulated Annealing and Differential Evolution. *Energy* **2019**, *181*, 654–664. [[CrossRef](#)]
26. Xiao, Y.; Sun, T.; Cui, G. Enhancing strategy promoted by large step length for the structure optimization of heat exchanger networks. *Appl. Therm. Eng.* **2020**, *173*, 115199. [[CrossRef](#)]
27. Xiao, Y.; Cui, G.; Zhang, G.; Ai, L. Parallel optimization route promoted by accepting imperfect solutions for the global optimization of heat exchanger networks. *J. Clean. Prod.* **2022**, *336*, 130354. [[CrossRef](#)]
28. Ahmad, S. Heat Exchanger Networks: Cost Tradeoffs in Energy and Capital. Ph.D. Thesis, University of Manchester Institute of Science and Technology (UMIST), Manchester, UK, 1985.
29. Linnhoff, B.; Ahmad, S.J.C. Engineering, Cost optimum heat exchanger networks—1. Minimum energy and capital using simple models for capital cost. *Comput. Chem. Eng.* **1990**, *14*, 729–750. [[CrossRef](#)]
30. Yerramsetty, K.M.; Murty, C.V.S. Synthesis of cost-optimal heat exchanger networks using differential evolution. *Comput. Chem. Eng.* **2008**, *32*, 1861–1876. [[CrossRef](#)]
31. Khorasany, R.M.; Fesanghary, M. A novel approach for synthesis of cost-optimal heat exchanger networks. *Comput. Chem. Eng.* **2009**, *33*, 1363–1370. [[CrossRef](#)]
32. Zhang, H.; Cui, G.; Xiao, Y.; Chen, J. A novel simultaneous optimization model with efficient stream arrangement for heat exchanger network synthesis. *Appl. Therm. Eng.* **2017**, *110*, 1659–1673. [[CrossRef](#)]
33. Rathjens, M.; Fieg, G. A novel hybrid strategy for cost-optimal heat exchanger network synthesis suited for large-scale problems. *Appl. Therm. Eng.* **2020**, *167*, 114771. [[CrossRef](#)]
34. Xu, Y.; Cui, G.; Han, X.; Xiao, Y.; Zhang, G. Optimization route arrangement: A new concept to achieve high efficiency and quality in heat exchanger network synthesis. *Int. J. Heat Mass Transf.* **2021**, *178*, 121622. [[CrossRef](#)]
35. Chen, J.; Cui, G.; Shen, S. An polymorphic firefly algorithm with self-adaptation strategy for process system heat integration. *Case Stud. Therm. Eng.* **2023**, *47*, 103116. [[CrossRef](#)]
36. Ahmad, S.; Patela, E. SUPERTARGET: Applications software for oil refinery retrofit. In Proceedings of the American Institute of Chemical Engineers Spring National Meeting, Houston, TX, USA, 29 March 1987.

37. Liu, X.W.; Luo, X.; Ma, H.G. Studies on the retrofit of heat exchanger network based on the hybrid genetic algorithm. *Appl. Therm. Eng.* **2014**, *62*, 785–790. [[CrossRef](#)]
38. Liu, P.; Cui, G.; Xiao, Y.; Chen, J. A new heuristic algorithm with the step size adjustment strategy for heat exchanger network synthesis. *Energy* **2018**, *143*, 12–24. [[CrossRef](#)]
39. Sorsak, A.; Kravanja, Z. MINLP retrofit of heat exchanger networks comprising different exchanger types. In Proceedings of the 12th European Symposium on Computer Aided Process Engineering (ESCAPE-12), The Hague, The Netherlands, 26–29 May 2002; pp. 349–354.
40. Pavao, L.V.; Costa, C.B.B.; da Silva Sá Ravagnani, M.A. Automated heat exchanger network synthesis by using hybrid natural algorithms and parallel processing. *Comput. Chem. Eng.* **2016**, *94*, 370–386. [[CrossRef](#)]
41. Xiao, Y.; Cui, G.; Sun, T.; Chen, J. An integrated random walk algorithm with compulsive evolution and fine-search strategy for heat exchanger network synthesis. *Appl. Therm. Eng.* **2018**, *128*, 861–876. [[CrossRef](#)]
42. Zhang, H.; Cui, G. Optimal heat exchanger network synthesis based on improved cuckoo search via Lévy flights. *Chem. Eng. Res. Des.* **2018**, *134*, 62–79. [[CrossRef](#)]
43. Xu, Y.; Cui, G.; Deng, W.; Xiao, Y.; Ambonisye, H.K. Relaxation strategy for heat exchanger network synthesis with fixed capital cost. *Appl. Therm. Eng.* **2019**, *152*, 184–195. [[CrossRef](#)]
44. Caballero, J.A.; Pavão, L.V.; Costa, C.B.B.; da Silva Sá Ravagnani, M.A. A Novel Sequential Approach for the Design of Heat Exchanger Networks. *Front. Chem. Eng.* **2021**, *3*, 733186. [[CrossRef](#)]
45. Chang, C.; Liao, Z.; Costa, A.L.H.; Bagajewicz, M.J. Globally optimal synthesis of heat exchanger networks. Part III: Non-isothermal mixing in minimal and non-minimal networks. *AIChE J.* **2021**, *67*, 17393. [[CrossRef](#)]

**Disclaimer/Publisher's Note:** The statements, opinions and data contained in all publications are solely those of the individual author(s) and contributor(s) and not of MDPI and/or the editor(s). MDPI and/or the editor(s) disclaim responsibility for any injury to people or property resulting from any ideas, methods, instructions or products referred to in the content.